Nanostructured Copper Selenide Coatings for Antifouling Applications

Sergio Mancillas-Salas , José Ángel Ledón-Smith , Marissa Pérez-Álvarez * , Gregorio Cadenas-Pliego * , José Manuel Mata-Padilla , Marlene Andrade-Guel , Sandra Cecilia Esparza-González , Gregorio Vargas-Gutiérrez , Uriel Alejandro Sierra-Gómez , Esmeralda Monserrat Saucedo-Salazar

Posted Date: 1 December 2023

doi: 10.20944/preprints202312.0047.v1

Keywords: antimicrobial activity; nanoparticles synthesis; copper selenide

Article

Nanostructured Copper Selenide Coatings for Antifouling Applications

S. Mancilla-Salas [1], J.A. Ledón-Smith [1], M. Pérez-Alvarez [1,*] G Cadenas-Pliego [1,*], J.M. Mata-Padilla [2], M. Andrade-Guel [1], S.C. Esparza-González [3], G. Vargas-Gutiérrez [4], U.A. Sierra-Gómez [1] and E.M. Saucedo-Salazar [1]

[1] Centro de Investigación en Química Aplicada, Blvd. Enrique Reyna 140, Saltillo, Coahuila, 25294, México; sergio.mancilla.ps@ciqa.edu.mx; jangel.ledon.m20@ciqa.edu.mx; marissa.perez@ciqa.edu.mx; gregorio.cadenas@ciqa.edu.mx; marlene.andrade@ciqa.edu.mx; uriel.sierra@ciqa.edu.mx esmeralda.saucedo@ciqa.edu.mx;

[2] CONAHCYT-Centro de Investigación en Química Aplicada, Blvd. Enrique Reyna 140, Saltillo, Coahuila, 25294, México; jose.mata@ciqa.edu.mx;

[3] Universidad Autónoma de Coahuila, Saltillo, Coahuila, México; sceciliaesparza@gmail.com

[4] Centro de Investigación y de Estudios Avanzados del IPN, CINVESTAV Unidad Saltillo, Ramos Arizpe 25900, México. gregorio.vargas@cinvestav.edu.mx

* Correspondence: M. P-A marissa.perez@ciqa.edu.mx; G.C-P gregorio.cadenas@ciqa.edu.mx)

Abstract: The accumulation of microorganisms, plants, algae, or small animals on wet surfaces that have a mechanical function causes biofouling, which can result in structural or other functional deficiencies. The maritime shipping industry must constantly manage biofouling to optimize operational performance, which is a common and long-lasting problem. It can occur in any metal structure in contact or submerged in ocean water, which represents additional costs in terms of repairs and maintenance. This study is focused on the production of antifouling coatings, made with nanoparticles of copper selenide (CuSe) modified with gum arabic, within a water-base acrylic polymeric matrix. During the curing of the acrylic resin, the CuSe NPs remain embedded in the resin but this does not prevent the release of ions. The coatings presented to release copper and selenium ions for up to 80 days, selenium was the element that was released the most. The adhesion of film coatings to metallic substrates showed good adhesion, scale 5B (ASTM D3359 standard). Antimicrobial activity tests show that the coatings have an inhibitory effect on *Escherichia coli* and *Candida albicans*. The effect being more noticeable when the coating is detached from the substrate and placed on a growing medium, than compared to the coating on a substrate. Scanning electron microscopy (SEM) observations show that nanostructured CuSe coatings are made up of rod-shaped and spherical particles whose range ranges from 12 to 25 nm. The Energy Dispersive X-ray spectroscopy (EDS) studies showed that the ratio of selenium nanoparticles is greater than that of copper and that their distribution is homogeneous.

Keywords: copper selenide; antimicrobial activity; nanoparticles synthesis

1. Introduction

Biofouling can be defined as the adhesion of micro and macro-organisms to a metallic structure submerged in oceanic waters [1]. Its main consequence is the deterioration of the affected metals, derived from the corrosion induced by microorganisms (MIC), a fact that causes damage and weakening of the structures, increasing maintenance costs and their periodicity [2]. It is estimated that the damage associated with corrosion per year ranges from 30 to 50 billion dollars [3].

Biofouling is also associated with the increase in the use of fuel from ships, and its consequent increase in environmental pollution, due to the increase in friction during their displacement, studies establish that biofouling can increase fuel consumption between 40 and 77% [3]. An analysis of the economic impact of biofouling in the US Navy fleet indicates an additional cost of between $180-260 million US dollars per year [4]. A study evaluated the advantages of using antifouling coatings on yachts, considering the reduction in fuel consumption and the corresponding reduction in CO_2

 doi:10.20944/preprints202312.0047.v1

emissions. It was found that approximately the fuel reduction in one year can be 13.7 x 10^3 kg and CO_2 emissions can be reduced by 43.3 tons [5].

Other damages caused by biofouling is the blockage of drainage pipes, or those presented by oil or power generation off-shore platforms, which become heavier and less resistant to marine wear [6]. Another important consequence of the formation of the biofouling would be the ecological alteration caused by the artificial introduction of organisms (through dragging) from one ecosystem to another [4, 7].

The prevention of biofouling phenomena is a widespread issue dealing with a plethora of research fields focused on the design of highly performing nanocomposite materials. The quest for suitable fouling resistant surfaces involves water purification systems, marine equipment, biomedical devices, food packaging, fabrics, and heritage materials [1, 8, 9].

The increasing interest in the development of antifouling coatings, has led to the development of different types of coatings that are used today. Decades ago, coatings made with paints embedded cytotoxic agents were freely employed , whose function was the gradual release of these agents into the environment , but their use was restricted/limited due to the environmental deterioration they cause [10]. Coatings that facilitate removal (foul-release) have a hydrophobic surface where aquatic organisms have low adherence, which facilitates their removal. Some of these coatings can be gradually hydrolyzed, releasing their surface layer, thus limiting biofouling [11, 12]. Finally, another type of antifouling coatings are those that usually employ a polymer matrix endowed with nanoparticles, which in combination have an effect that limits or inhibits microbial growth [13]. In addition, the surface roughness characteristics of these coatings are also a limitation for biofouling [14].

The type of nanoparticles and their interaction with the polymer matrix are the main factors to consider in the development of antifouling coatings. The use of copper as an antimicrobial agent has been known since antiquity and its use as nanoparticles is well documented [15, 16]. In the last decade the interest in synthesizing copper nanoparticles [1, 17] and copper nanocomposites has increased significantly [18-21], since their excellent properties allow them to have applications in different fields of science.

Selenium is an element with biological importance, since forms part of most living beings, it has low toxicity and excellent antimicrobial properties, it is used in various products related to the safety of human health, for example in the generation and handling of food [8, 22, 23], as an antioxidant [24, 25], for its anti-carcinogenic properties [25], and therapeutical applications [26], among others.

Copper selenide (CuSe), on the other hand, is a chalcogenide commonly used in applications such as photovoltaics, thermoelectrics and electronics [27-29]. It is a compound capable of being presented in different compositions and stoichiometries [28, 29, 30]. Few has been said about its antimicrobial properties but considering that copper and selenium present excellent antimicrobial properties separately, CuSe may be a promising candidate in this field.

In the present work, we develop nanostructured antifouling coatings that consist of copper selenide (CuSe) nanoparticles and a commercial acrylic resin Rhoplex Ac-261 and were evaluated their surface, mechanical and antimicrobial properties.

2. Materials and Methods

2.1. CuSe nanoparticles synthesis.

The chemical synthesis of CuSe nanoparticles was carried out in our work group using a similar methodology previously reported [24]. In a 2L capacity glass reactor, 1.25L of distilled water and 3.0 g of gum arabic (GA) were introduced and stirred to 200 rpm during 15 min. Then, 5.2g of H_2SeO_3 were added to the mixture and the stirring was incremented to 330 revolutions per minute (rpm) to ensure that the reaction was homogeneous, stirring was maintained for 50 min. Then, a solution of $CuSO_4 \cdot 5H_2O$ (0.16 M) was added to reaction mixture. At this point the reactor is hermetically closed, and the stirring was incremented to 400 rpm. After, 9 mL of hydrazine (N_2H_4) were added dropwise and the reactor stirring maintained for another 60 min. The mixture reaction solution was separated

 doi:10.20944/preprints202312.0047.v1

by centrifugation at 8500 rpm during 30 min at room temperature. The collected black solid products were washed twice with distilled water and ethanol and dried under vacuum at 60°C for 1 h. The molar ratio Se/Cu used in this project was 1.24.

2.2. Preparation of nanostructured CuSe nanoparticles coatings.

For the preparation by deposition of the nanostructured coatings, the substrates were first treated to eliminate oxides, deformations and defects by surface blasting following the ASTM-G5 standard. First, abrasive papers of the following grain sizes were used: 280, 400, 600, 800 and 1000. They were used from the largest grain size to the smallest, ensuring a mirror polished, necessary for the correct adhesion of the nanostructured coatings, they were abraded both faces and corners of the substrates. The process was carried out wet, using deionized water to achieve the mirror polished. Once the mirror polished was achieved, the samples were washed with deionized water and placed in a 10% NaOH solution for 7 minutes, to remove fats and contaminants. that were on its surface that could somehow prevent the coating resin from adhering properly. They were washed first with plenty of deionized water and finally with ethanol, and then allowed to air dry. The treated substrates were used in less than 24 hours after drying, to avoid the formation of oxides.

The preparation of the formulations was performed in two steps. First, it consisted of suspending the nanoparticles in water, due to the nature of the nanoparticles this step required the use of ultrasound equipment, the conditions were established at 70 kHz for a time of 15 minutes, then the solution was allowed to cool for a few minutes monitoring the dispersion of the nanoparticles in the medium. The second step consisted of adding the solution at room temperature to the resin to form the nanostructured coating. This required mixing it in a reactor (Parr, 4842) at approximately 400 rpm for 10 minutes to ensure correct mixing.

Optical microscopy was used to analyzed the coatings and observe the microstructure of the nanoparticles, for this an optical microscope at 4x magnification lens was employed.

Fourier transformed infrared spectroscopy (FTIR) was performed with a Thermo Scientific Nicolet iS20 using an ATR.

A scanning electron microscope (SEM) was used to analyze the microstructure, a sample was prepared by applying a coating formulation composed of commercial resin, water and 3.0% by weight of CuSe nanoparticles on a 1mm x 1mm stainless steel substrate. The sample was coated with gold and palladium before analysis. The technique was carried out in a Jeol brand JSM-7001F scanning electron microscope operated at 8kV.

For ion release analysis, a sample of the coating was placed in a flask with 20 mL of distilled water. The jar was closed, and the coatings were kept at rest for 5, 10, 20, 40, and 80 days. Subsequently, the water of all flasks was analyzed by inductively coupled plasma (ICP) (Thermo Scientific, ICAP PRO DUO). Distilled water was used as a blank. The swollen samples, 5, 10, 20, 40 and 80 days, were dried at room temperature. These samples underwent a surface roughness analysis, and the contact angle was measured.

Coatings roughness was measured by a Keyence VR Series profilometer. Contact angle measurements were performed by a Rame-Hart goniometer using 3 μL of distilled water in each measurement.

2.4. Mechanical performance tests.

The adhesion of nanostructured CuSe coatings to the stainless-steel substrate was determined based on the ASTM D3359 standard (American Standard Test Methods for Measuring Adhesion by Tape Test). As stablished by the test, a lattice pattern with eight cuts are made in each direction through the film to the substrate, pressure sensitive tape is applied to the web pattern and then removed, and qualitative adhesion is assessed on a scale of 0 to 5B.

 doi:10.20944/preprints202312.0047.v1

2.5. Microbiological test.

For the antimicrobial tests, colonies of: *Escherichia coli* (Gram negative bacteria) and *Candida albicans* (fungi) were used. Nutrient agar (BD Bioxon) was employed, prepared according to the product instructions. Subsequently, the culture medium was sterilized in an autoclave at a temperature of 121°C and 15 psi of pressure for 15 minutes. Finally, it was cooled at room temperature, until it reached room temperature.

CuSe nanostructured coatings were prepared at concentrations of 0, 0.5, 1.0, 1.5, 2.0 and 3.0% weight of CuSe nanoparticles (2 for each concentration), and the culture medium was applied directly to the coatings. Subsequently, on the surface of each agar, a perforation was made where 10 µL of inoculum were poured (each inoculum for all 6 concentrations). Finally, these samples were incubated for 24 hours.

To validate these results, a special test was carried out, using only the coating without the substrate (a thin film). New culture mediums were prepared and inoculated with both microorganisms, then the thin film was placed on the inoculated agar. Concentrations used were the same as before, obtaining 12 treatments. Similarly, the samples were incubated for 24 hours and then observed in an optical microscope at 40x.

3. Results and discussion

3.1. CuSe nanoparticles coatings characterization

Error! Reference source not found. presents the optical image of CuSe antifouling coating at 4x. It can be appreciated that this coating presents a not homogeneous distribution due to the formation of bubbles during drying and curing of the coating. Imperfections on the surface can be observed even when different layers of the coating are applied.

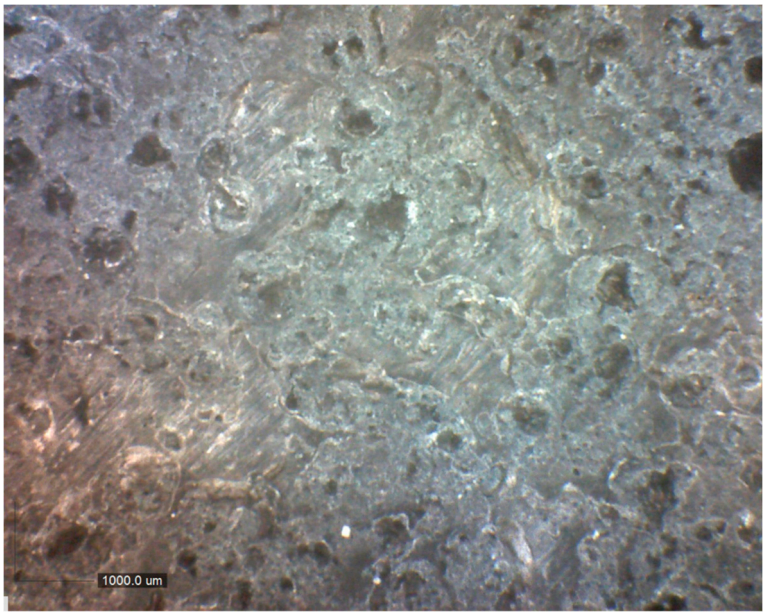

Figure 1. Optical image of CuSe antifouling coating at 4x.

Error! Reference source not found. presents the FTIR spectra of CuSe nanoparticles antifouling coating and the Rhoplex Ac-261 commercial resin as a blank. Rhoplex Ac-261 acrylic resin spectrum presents bands between 3000-2800 cm^{-1}, 1730 cm^{-1} and 1030-1250 cm^{-1}, which can be assigned to bands of C-H bonds, carbonyl groups and C-O respectively. The detailed analysis of the spectrum shows characteristic signals at 2958 cm^{-1}, 2882 cm^{-1}, 1730 cm^{-1}, 1448 cm^{-1} and 1152 cm^{-1}, where the first two are attributed to stretching of the -CH group, while the third one belongs to the stretching of the C=O group and the fourth signal is due to stretching of the -CH_3 group as well as the last one is due to the stretching and vibrations of O-CH_3 corresponding to the ester group. The presence of the band at

 doi:10.20944/preprints202312.0047.v1

3446 cm^{-1} suggests the presence of hydroxyl groups (-OH) or water molecules trapped in the test material [31]. The bands described are characteristic of polymethylmethacrylate (PMMA), however, the absorption band at 961 cm^{-1} is typical of polybutylacrylate (PBA), this band is due to the oscillation of the carbon of the -COO group of the PBA, as found in the literature [32]. PMMA and PBA had similar molecular backbones, only slight differences were found in their FTIR spectra, the presence of these segments suggests the presence of the copolymer P(MMA-co-BA) [33].

The spectrum of the nanostructured coating with CuSe nanoparticles turned out to be very similar, the main difference found is the peak localized at 611 cm^{-1}, which is attributed to bending vibrations of CuSe [29]. Modifications and shifts in the nanostructured CuSe coating spectrum compared to the Rhoplex Ac-261 spectrum are attributed to an interaction with CuSe-GA nanoparticles. As reported, predominant groups of gum arabic can be shown in the spectrum of the modified nanoparticles [34].

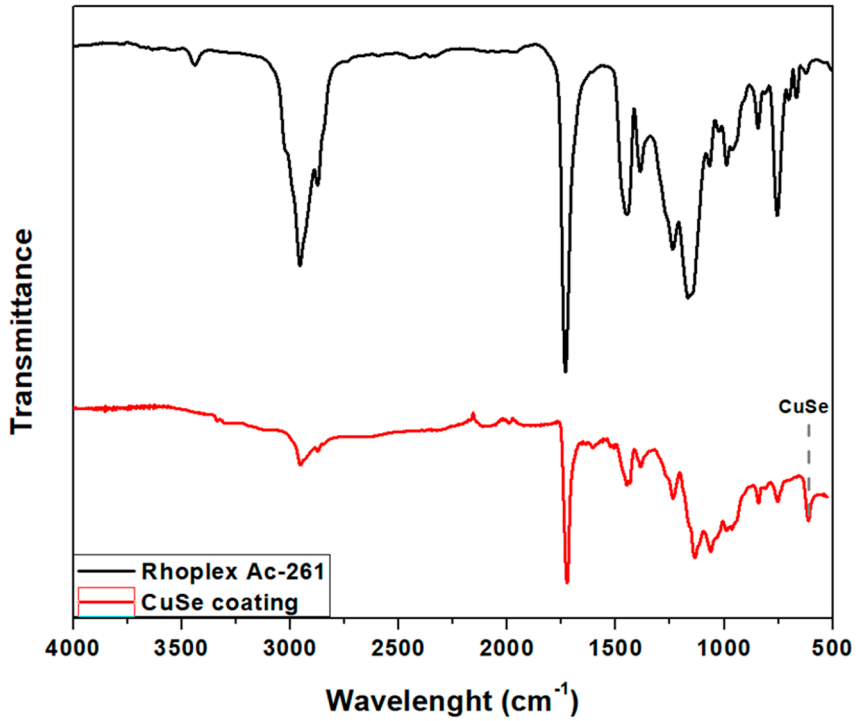

Figure 2. FTIR spectra of CuSe nanoparticles coating, and Rhoplex Ac-261 commercial.

Error! Reference source not found. shows the SEM micrograph of coated with antifouling solution for elemental analysis. In this analysis, five zones were selected to carry out the elemental analysis, zones 1, 2 and 3 were the ones that presented a greater number of particles compared to zone 4 and 5.

Preprints (www.preprints.org) | NOT PEER-REVIEWED | Posted: 1 December 2023 doi:10.20944/preprints202312.0047.v1

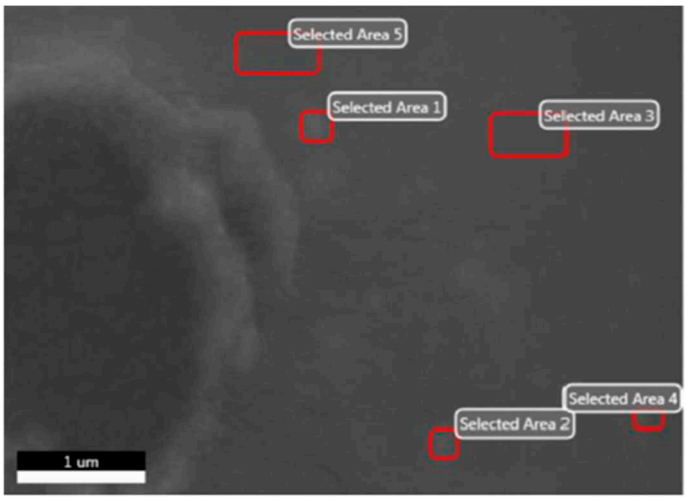

Figure 3. SEM micrograph of the substrate coated with antifouling solution for elemental analysis.

According to the analysis, the presence of copper and selenium was observed in all areas. This demonstrates that the copper and selenium particles are embedded in the resin and that the dispersion and depth of the particles is varied.

shows a comparison of Rhoplex Ac-261 commercial resin and the spectrum obtained from the elemental analysis, where the signals that are not labeled correspond to the elements gold and palladium used in the preparation of the sample.

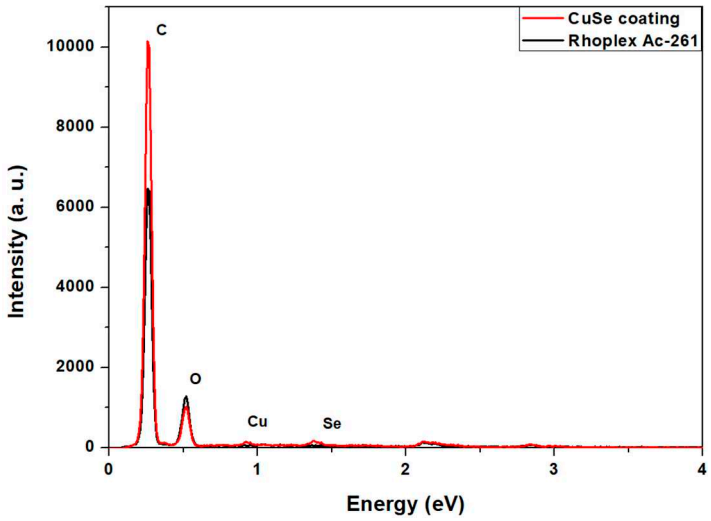

Figure 4. EDAX analysis of the nanostructured coating.

Error! Reference source not found. shows the concentration in weight percentage of the elements carbon, oxygen, selenium, and copper. The average of the first three zones showed that the amount of selenium in the coating was greater than the amount of copper (Se/Cu =1.35); on the other hand, the elements carbon and oxygen come from the chemical structure and functional groups of the resin and the gum arabic.

Table 1. Weight percent of element concentrations in CuSe nanostructured coatings.

Element	Wt. %
Oxygen	77.4
Carbon	20.62
Selenium	1.14

 doi:10.20944/preprints202312.0047.v1

Copper	0.84

On the other hand, elemental mapping was carried out to determinate the presence of copper and selenium nanoparticles in the coating. In **Error! Reference source not found.**a yellow dots are observed, which represent selenium particles. In the right area of the image, the presence of these points was not observed because the substrate has a hole in this area. Similarly, in **Error! Reference source not found.**b, blue dots are observed, which correspond to copper particles. Both analyzes were carried out in the same area of the substrate. Comparing figures, it was observed that the amount of copper particles present in the substrate is less than the amount of selenium particles, this agrees with their weight percentages presented in **Error! Reference source not found.**.

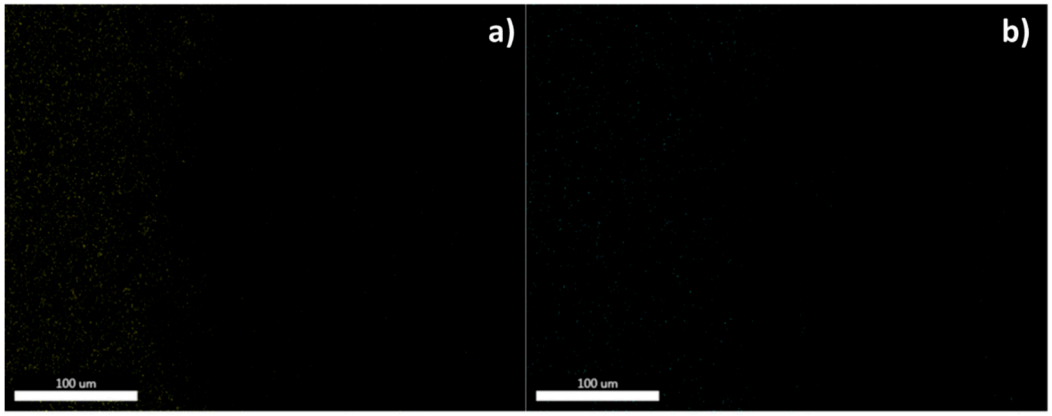

Figure 5. Elemental mapping of nanostructured CuSe coatings a) selenium, b) copper.

Scanning electron microscopy micrographs at 50,000x and 100,000x are shown in **Error! Reference source not found.**a and **Error! Reference source not found.**b, respectively. In both magnifications they show two types of morphologies: rod-shaped nanoparticles and spherical nanoparticles. The nanoparticles with spherical morphology have an average diameter in the range of the 32.1 nm and 49.8 nm, while rod-shaped nanoparticles mainly presented longitudes de around 101.6 nm. Although both types of nanoparticles showed a tendency to form agglomerates, it was not possible to observe micron-sized agglomerates where the nanoparticles fused, and the original spherical morphology could not be observed.

It has been reported that selenium and CuSe nanoparticles are structurally unstable and can change their size and morphology depending on the synthesis conditions, causing the formation of micrometric agglomerates; the transformation can occur at low temperatures such as 70°C. This phenomenon was not observed in the coatings with CuSe nanoparticles even though they were subjected to temperatures of 130°C during curing.

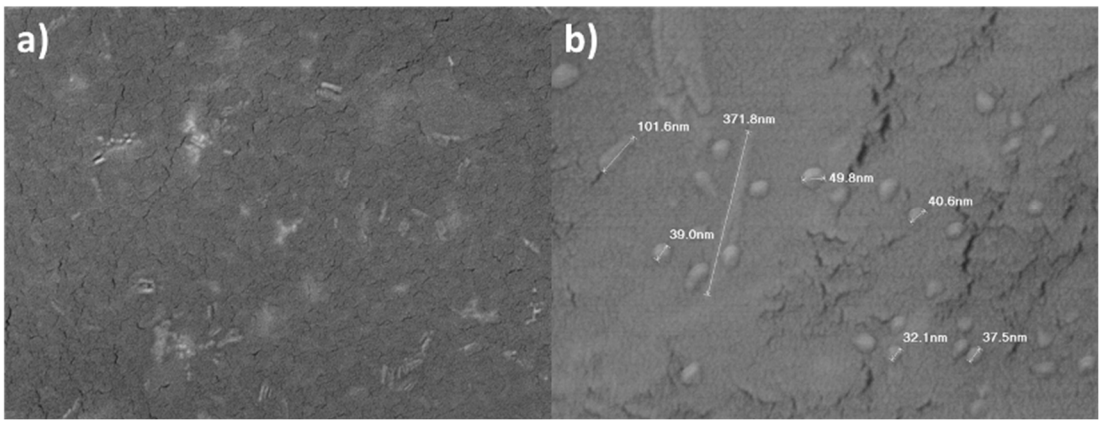

Figure 6. Scanning electron micrographies of CuSe nanostructured coatings at 3.0% wt. of CuSe nanoparticles. a) Magnification at 50 000x, b) magnification at 100 000x.

 doi:10.20944/preprints202312.0047.v1

Error! Reference source not found. presents the results of ion release tests elemental analysis. The results show that the nanoparticles were able to release ions through the polymer matrix and as the exposure time increases the ion release also increases. A clear tendency can be seen in the release of ions, with selenium been released in a higher concentration in all cases, with respect to copper.

The phenomenon of ion release from nanoparticles embedded in a polymer matrix is achieved in several stages, but mainly 3 are involved in soluble matrices, which are:

1.- The release by "burst": this occurs when the ions that are closest to the surface are released, this could be due to a release due to swelling of the material [35], to the bad interaction between the matrix and the active principle or by the porosity of the matrix when it comes into contact with an environment that dissolves it [36].

2.- The diffusional release: it is the stage where the ions begin to diffuse through the polyacrylate matrix [35, 37].

3.- Erosional release: this occurs when the material degrades due to environmental causes, which releases ions [35, 37].

For systems with nanoparticles homogeneously distributed in the medium, only the last two stages are considered, while for those that are heterogeneously distributed, all three occur. For this case, it is considered that the nanoparticles are homogeneously distributed and settled on the coating surface.

Between days 40 and 80, the release of selenium ions decreased, this can be due to many factors as follows. First, the substrate could be presenting limitations of ion release, where there could be erosion or diffusion through the membrane. Another explanation could be that at a time point between 20 and 80 days of exposure there is an impediment in the release of selenium ions because they are bonded as a compound with copper in addition to the fact that, as previously reported, the use of biopolymers as stabilizers in nanoparticles could slow down the release of these [38].

The results obtained in the release of ions from the coating show that the release occurs very slowly. This release rate suggests that there is a good interaction between the resin and the CuSe-GA nanoparticles, since if there were weak interactions between them, we would observe a sudden initial release [36, 39], which is not optimal for applications such as coatings or paintings. These results are in agreement with the finding found in FTIR, where a shift of the bands was presented due to this type of interactions.

Table 2. Ion release tests elemental analysis.

Sample supernatant	Se (ppm)	Cu (ppm)
Blank (distilled water)	0	0
Black 5 days	0.088	0.009
Black 10 days	0.125	0.014
Black 20 days	0.414	0.034
Black 40 days	0.737	0.047
Black 80 days	0.519	0.132

Error! Reference source not found. presents the surface roughness of nanostructured CuSe nanoparticle coatings. Arithmetic mean height (Sa) starts with a value of 17.0 μm and increases to 117.3 μm after 10 days. From here, a decreased in the arithmetic mean is recorded, reaching 85.2 μm at 80 days.

On the other hand, the maximum height obtained (Sz) exhibits a behavior similar to the previous one, which confirms having the maximum height at 10 days and after that a decreased in both coatings.

This observed behavior may be due to the interaction of water with the coating. In the first days of immersion, the coating tends to swell, which under the roughness analysis; indicates an increase in it.

After 10 days, the maximum peak of roughness is observed, which would correspond to the maximum capacity of the coating to swell due to water, and from there; The coating begins to return

Preprints (www.preprints.org) | NOT PEER-REVIEWED | Posted: 1 December 2023 doi:10.20944/preprints202312.0047.v1

to its previous shape, so it gradually returns to its previous shape. The fact that the coating does not recover its original roughness indicates that the interaction with water generates an irreversible increase in roughness.

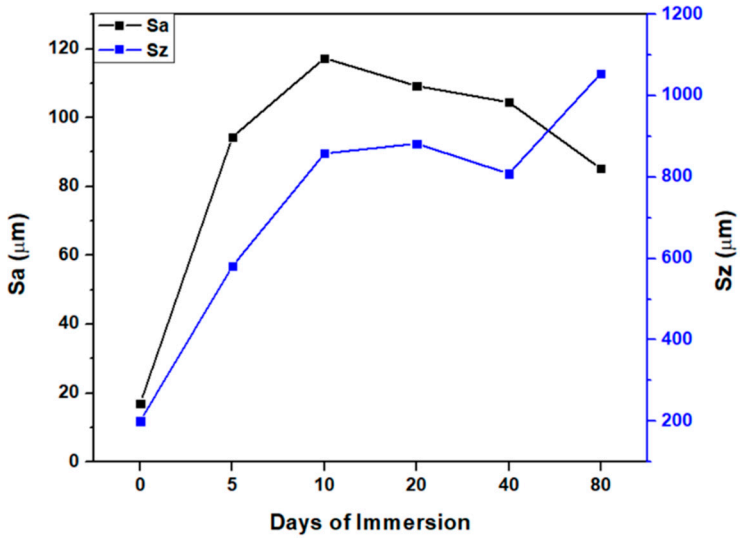

Figure 7. Surface roughness analysis of CuSe nanostructured coatings, arithmetic mean height (Sa), and maximum height (Sz).

Figure 8. presents the contact angle measurements of nanostructured CuSe coatings. The measurement of the contact angle of nanostructured CuSe coating without water immersion (0 days) was 39.6 degrees. At 5, 10, and 20 days, different values of 75, 74, and 78 degrees were observed. These results indicate that the changes obtained in the surface of the nanostructured CuSe coating by immersion tend to exhibit a decrease in their hydrophilic behavior. However, at 40 and 80 days, there is a decrease in contact angle of 49 and 51 degrees, respectively, indicating that the hydrophilic character increase after 20 days of immersion.

These coatings show a minor hydrophilic character between 5 and 20 days, indicating that immersion during the first days significantly alters their nature. The fact that this character is lost after 20 days suggests that the coating returns to a state similar to the initial one, and therefore that it recovers its hydrophilic character [40]. This experimental evidence explains the strong release of selenium and copper ions observed after 20 days.

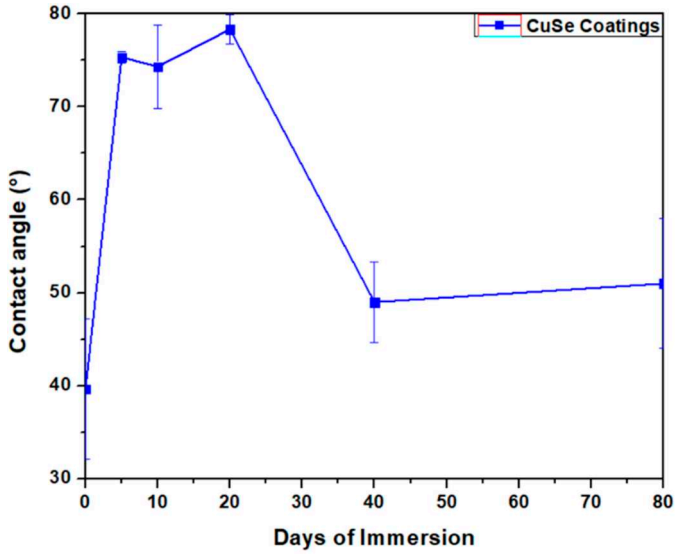

Figure 8. Contact angle measurements of nanostructured CuSe coatings.

 doi:10.20944/preprints202312.0047.v1

3.2. Mechanical tests analysis

Error! Reference source not found. presents the nanostructured CuSe coatings measuring adhesion probe by tape test results. It can be appreciated that after scratching and adhesion of the tape, the coating is maintained (having only detachment in the scratched area). Which places it in a 5B rating, this being the highest. This indicates that the adhesion of these coatings is high, so it is expected that they do not come off easily under uncontrolled conditions.

We want to strongly emphasize that CuSe-coated steel substrates can be mechanically cut without peeling off the coating.

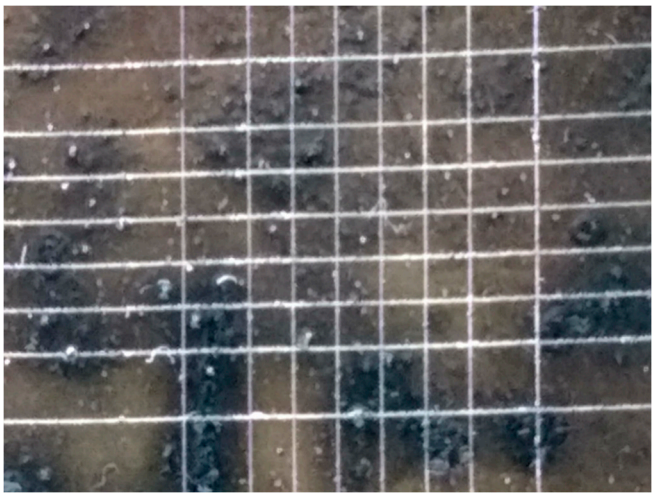

Figure 9. Nanostructured CuSe coatings measuring adhesion probe by tape test results.

3.3. Microbiological tests results

The results of microbiological analyses of nanostructured CuSe coatings are shown as follow. First, **Error! Reference source not found.** images consist of CuSe nanostructured coatings at different weight concentrations of CuSe nanoparticles covered with the culture medium (without inoculation). These coatings will serve as a target to compare with the inoculated coatings, in order to compare color, texture and possible microbial growth. The culture medium has a transparent, slightly yellow appearance. However, as the concentration of CuSe nanoparticles increases, the slightly yellow appearance becomes slightly darker. It is observed that there is no evidence of microbial growth.

Error! Reference source not found.11 and **Error! Reference source not found.** exhibit microbial growth of both strains *E. coli* and *C. albicans* in contact with nanostructured coatings at different CuSe concentrations.

 doi:10.20944/preprints202312.0047.v1

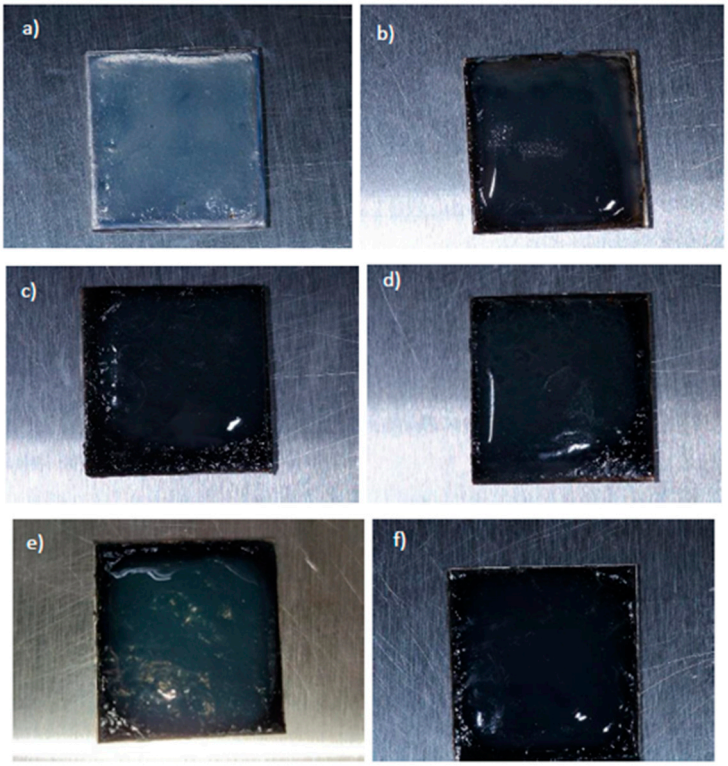

Figure 10. Nanostructured CuSe coatings a) 0, b) 0.5, c) 1, d) 1.5,.e) 2 and f) 3% wt. with nutrient agar.

In **Error! Reference source not found.** we can observe images that show the nanostructured CuSe coatings inoculated with *Escherichia coli*. Comparing **Error! Reference source not found.**a and **Error! Reference source not found.**a, it can be seen that **Error! Reference source not found.**a shows a yellow coloration and a milky white halo around the inoculation zone, indicating that there is microbial growth in the target. On the other hand, in the other figures (**Error! Reference source not found.**b-f) a significant color change is not observed in the color of the culture medium, nor is the milky white halo around the inoculation zone. These results suggest that CuSe nanostructured coatings in concentrations of 0.5 to 3.0% by weight of CuSe nanoparticles have an inhibitory effect on the growth of *E. coli* on nutrient agar.

Preprints (www.preprints.org) | NOT PEER-REVIEWED | Posted: 1 December 2023 doi:10.20944/preprints202312.0047.v1

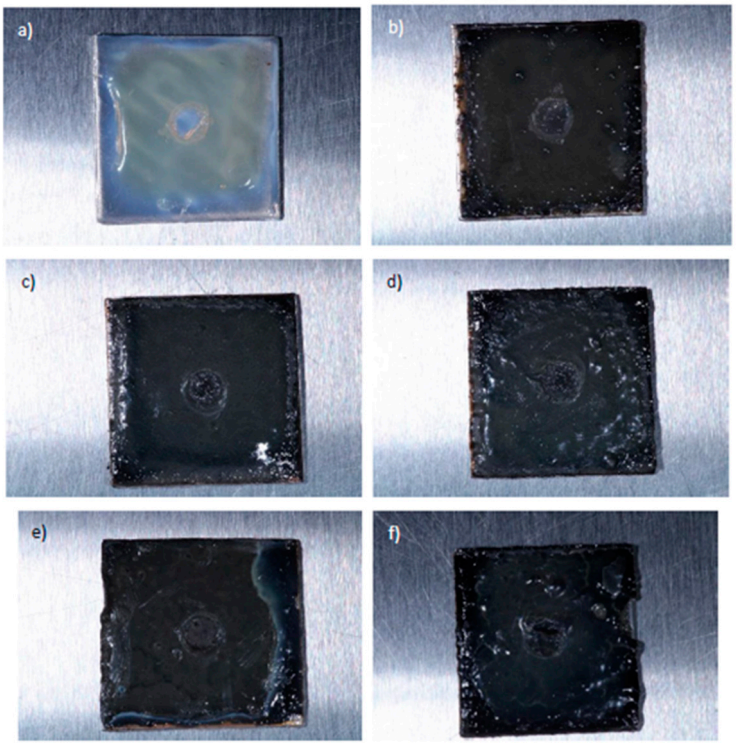

Figure 11. Nanostructured CuSe coatings a) 0, b) 0.5, c) 1.0, d) 1.5, e) 2.0 and f) 3.0% wt. inoculated with *Escherichia coli*.

Error! Reference source not found. presents nanostructured CuSe coatings inoculated with *Candida albicans* studied under the same conditions as the bacteria *Escherichia coli*.

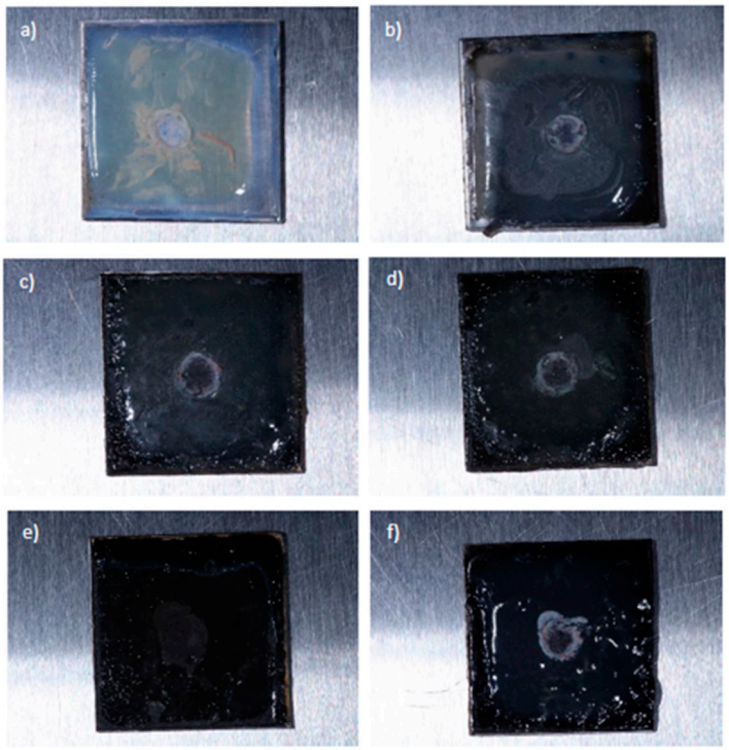

Figure 12. Nanostructured CuSe coatings a) 0, b) 0.5, c) 1.0, d) 1.5,. e) 2.0 and f) 3.0% wt. inoculated with *Candida albicans*.

 doi:10.20944/preprints202312.0047.v1

Error! Reference source not found. and **Error! Reference source not found.** present the photographic evidence of the direct contact between the nanostructured coatings and the agar. In this case, the coatings were removed in the form of a film from the metal substrates by scraping and placed directly in Petri dishes with nutrient agar inoculated with *Escherichia coli* and *Candida albicans*. The concentrations of CuSe nanostructured coatings employed were the same as the previous experiment, 0, 0.5, 1.0, 1.5, 2.0 and 3.0% wt. of CuSe nanoparticles. **Error! Reference source not found.** and **Error! Reference source not found.** show the presence of two zones separated by a central line, the zone located on the left corresponds to microbial growth under optimal conditions and the zone on the right corresponds to microbial growth in the presence of the nanostructured CuSe coating.

Error! Reference source not found. shows the images of nanostructured CuSe coatings at different concentrations at wt.% in the direct contact with the *E. Coli* strain. **Error! Reference source not found.**a works as a blank where no nanostructured coating was used.

On the side exposed to the nanostructured CuSe coatings, microbial growth is lower than on the opposite side. This inhibition increases as CuSe nanoparticles concentration increases, as seen in the imagen of CuSe 2.0 wt. %. and higher concentrations. These results match with the previous experiment, where the microbial growth inhibition caused by nanostructured CuSe coatings for *Escherichia coli* was demonstrated.

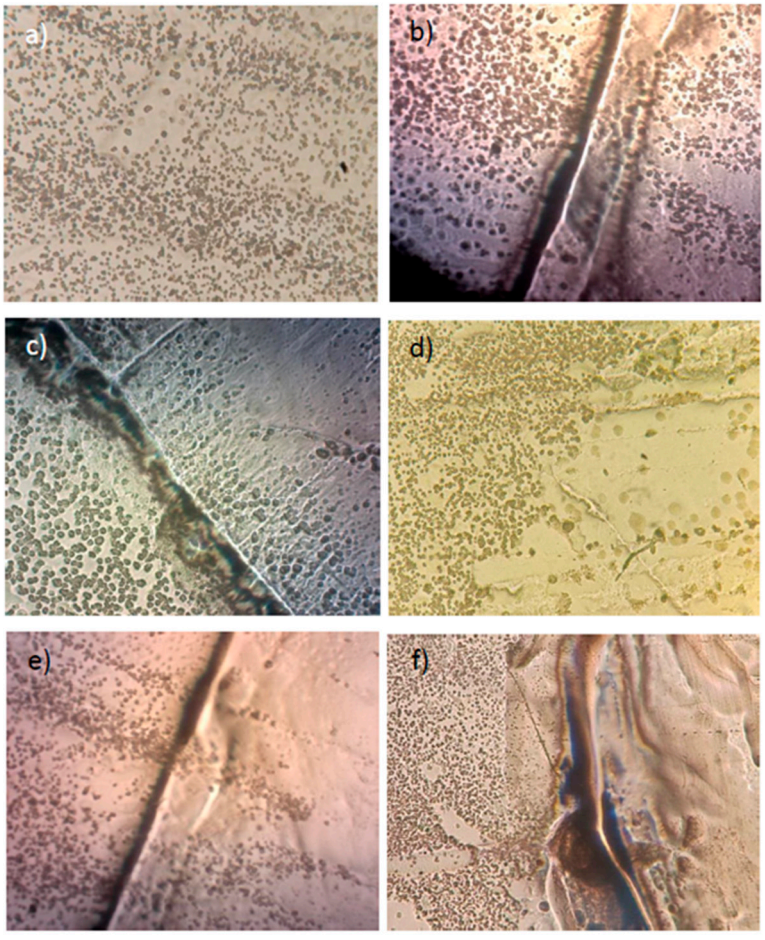

Figure 13. Images of the inhibition evaluation of direct contact of. nanostructured CuSe with *Escherichia coli* strain.

Error! Reference source not found. presents images of the inhibition evaluation of the direct contact of nanostructured CuSe coating with *Candida albicans* strain. **Error! Reference source not found.**a shows the image of the blank where no nanostructured CuSe coating was used.

As in the counterpart with *E. coli*, the inhibition produced by the CuSe nanostructured coatings can be appreciated. This inhibition is observed clearly in all the treatments and becomes clearer as

 doi:10.20944/preprints202312.0047.v1

the CuSe concentration increases. These results confirm that the nanostructured CuSe coatings have an inhibitory effect, in direct contact, on microbial growth on *Candida albicans*.

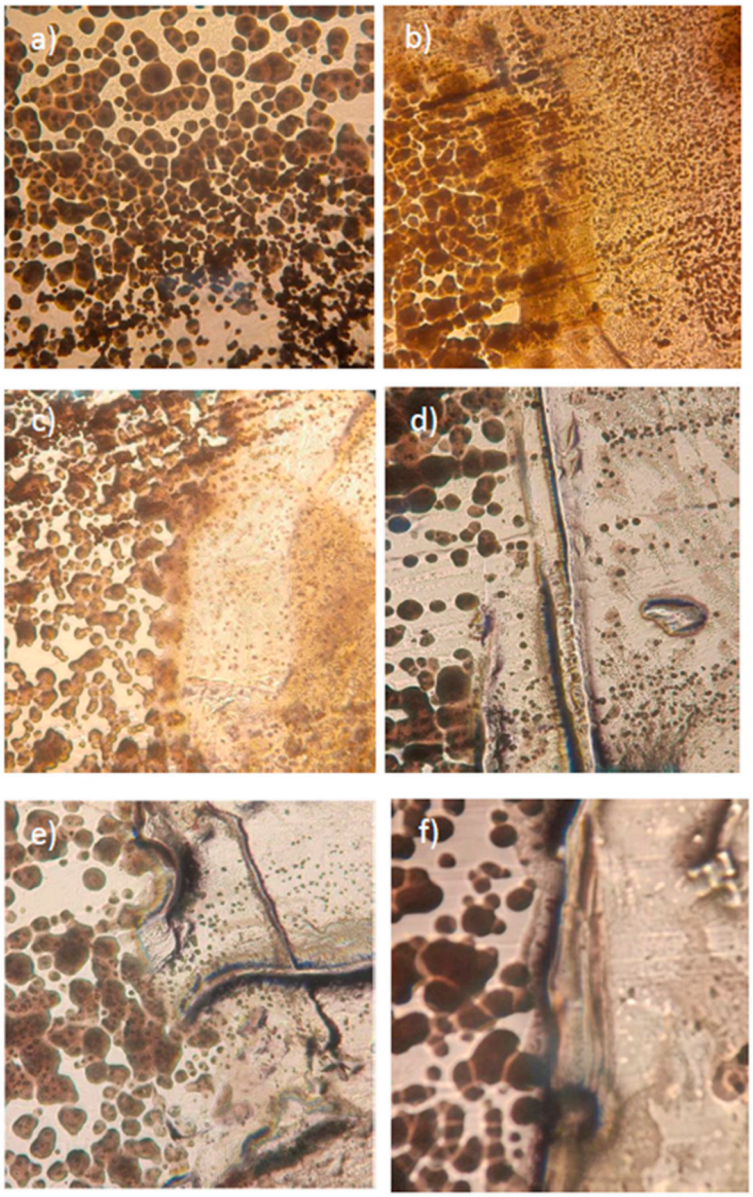

Figure 14. Inhibition evaluation of the direct contact of CuSe. nanostructured coating with *Candida albicans*.

4. Conclusions

Nanostructured CuSe antifouling coatings were successfully obtained employing previously synthesized CuSe nanoparticles modified with gum arabic, embedded in a commercial resin.

Despite the surface inhomogeneity of the coatings, the scratch adhesion tests showed great adhesion, in part, due to the interaction present among the CuSe nanoparticles, the gum arabic and the commercial resin determined by FTIR.

Elemental analysis using EDS shows that the nanostructured coating is composed mainly for oxygen and carbon, elements that belong to the resin and gum arabic. Besides these elements, selenium and copper appear. Selenium being in a higher proportion than copper. On the other hand, elemental mapping shows that both selenium and copper are well dispersed in the coating being selenium found in a higher proportion.

The micrographs obtained by electron microscopy show that the nanostructured CuSe coatings are composed of agglomerates of nanoparticles and semi-spherical and elongated particles whose length is between 12 and 25 nm.

The nanostructured CuSe coating was shown to have excellent adhesion (ASTM D3359 standard), rating of 5B, the highest (having only detachment in the scratched area). This result indicates that the mechanical properties of the coating are outstanding, so it would be expected to be very resistant and not easily detached under hostile environmental conditions.

Release of selenium and copper ions in these coatings was verified, where selenium ions were released in greater proportion. During the drying and hardening of the coating, the CuSe NPs remain embedded in the resin matrix, this process leads to good mechanical resistance of the coating and favors the slow release of the ions, which are responsible for the inhibition of microbial growth of the microorganisms studied *Escherichia coli* and *Candida albicans*.

Author Contributions: Conceptualization, M.P.A., G.C.P., J.M.M.P.; methodology, S.C.E.G, M.A.G, S.M.S., J.A.L.S.; validation, S.C.E.G, M.A.G, S.M.S., J.A.L.S.; formal analysis, G.V.G., U.S.G., E.M.S.S.; investigation, G.V.G., U.A.S.G., E.M.S.S.; resources, G.V.G., U.A.S.G., E.M.S.S; data curation, S.C.E.G, M.A.G, S.M.S., J.A.L.S.; writing—original draft preparation, S.M.S., M.P.A., G.C.P., J.M.M.P.; X.X.; writing—review and editing, M.P.A., G.C.P., J.M.M.P.; visualization, J.A.L.S., G.C.P.; supervision, G.C.P., J.M.M.P.; funding acquisition, G.C.P., J.M.M.P., G.V.G. All authors have read and agreed to the published version of the manuscript.

Funding: This research was funded by CONACyT-SENER-Sustentabilidad Energética, Centro Mexicano de Innovación en Energía del Océano Grant No. 0249795 and FORDECYT-PRONACES/845101/2020, grant number 845101 and APC was funden by FORDECYT-PRONACES/845101/2020, grant number 84510.

Institutional Review Board Statement: Not Applicable.

Data Availability Statement: The data presented in this study are available on request from the corresponding authors.

Acknowledgments: The authors kindly acknowledge the scholarship to Marissa Pérez-Alvarez (postdoctoral) and José Ángel Ledón Smith provided by CONAHCYT. The authors would also like to thank G. Mendez Padilla, A. Espinoza Muñoz, Maricela García Zamora, J.A. Mercado Silva, J. Campos Oyervides, M.d.R. Rangel Ramírez and Beatriz Reyes Vielma for their valuable technical support.

Conflicts of Interest: All the authors declare that they have no known competing financial interests or personal relationships that could have appeared to influence the work reported in this paper.

References

1. Jardón-Maximino, Noemi, Pérez-Alvarez, Marissa, Cadenas-Pliego, Gregorio, Lugo-Uribe, Luis E., Cabello-Alvarado, Christian, Mata-Padilla, José M. and Barriga-Castro, Enrique Díaz. Synthesis of Copper Nanoparticles Stabilized with Organic Ligands and Their Antimicrobial Properties. Polymers, 2021; 13: 2846.
2. Li, Yangfan and Ning, Chengyun. Latest research progress of marine microbiological corrosion and bio-fouling, and new approaches of marine anti-corrosion and anti-fouling. Bioactive Materials, 2019; 4: 189-195.
3. Yang, Wen Jing, Neoh, Koon-Gee, Kang, En-Tang, Teo, Serena Lay-Ming and Rittschof, Daniel. Polymer brush coatings for combating marine biofouling. Progress in Polymer Science, 2014; 39: 1017-1042.
4. Callow, James A. and Callow, Maureen E. Trends in the development of environmentally friendly fouling-resistant marine coatings. Nature Communications, 2011; 2: 244.
5. Venettacci, Simone, Ponticelli, Gennaro Salvatore, Tagliaferri, Flaviana and Guarino, Stefano. Environmental and Economic Impact of an Innovative Biocide-Free Antifouling Coating for Naval Applications. Materials, 2023; 16: 748.
6. Gu, Y., Yu, L., Mou, J., Wu, D., Xu, M., Zhou, P. and Ren, Y. Research Strategies to Develop Environmentally Friendly Marine Antifouling Coatings. Mar Drugs, 2020; 18.
7. Cao, Shan, Wang, JiaDao, Chen, HaoSheng and Chen, DaRong. Progress of marine biofouling and antifouling technologies. Chinese Science Bulletin, 2011; 56: 598-612.
8. Ao, B., Du, Q., Liu, D., Shi, X., Tu, J. and Xia, X. A review on synthesis and antibacterial potential of bio-selenium nanoparticles in the food industry. Front Microbiol, 2023; 14: 1229838.
9. Calabrese, Carla, La Parola, Valeria, Testa, Maria Luisa and Liotta, Leonarda Francesca. Antifouling and antimicrobial activity of Ag, Cu and Fe nanoparticles supported on silica and titania. Inorganica Chimica Acta, 2022; 529: 120636.

10. Howell, Dickon and Behrends, Brigitte. A review of surface roughness in antifouling coatings illustrating the importance of cutoff length. Biofouling, 2006; 22: 401-410.
11. Gittens, Jeanette E., Smith, Thomas J., Suleiman, Rami and Akid, Robert. Current and emerging environmentally-friendly systems for fouling control in the marine environment. Biotechnology Advances, 2013; 31: 1738-1753.
12. Buskens, Pascal, Wouters, Mariëlle, Rentrop, Corné and Vroon, Zeger. A brief review of environmentally benign antifouling and foul-release coatings for marine applications. Journal of Coatings Technology and Research, 2013; 10: 29-36.
13. Pistone, Alessandro, Scolaro, Cristina and Visco, Annamaria. Mechanical Properties of Protective Coatings against Marine Fouling: A Review. Polymers, 2021; 13: 173.
14. Poornima Vijayan, P., Formela, Krzysztof, Saeb, Mohammad Reza, Chithra, P. G. and Thomas, Sabu. Integration of antifouling properties into epoxy coatings: a review. Journal of Coatings Technology and Research, 2022; 19: 269-284.
15. Cioffi, Nicola, Torsi, Luisa, Ditaranto, Nicoletta, Tantillo, Giuseppina, Ghibelli, Lina, Sabbatini, Luigia, Bleve-Zacheo, Teresa, D'Alessio, Maria, Zambonin, P. Giorgio and Traversa, Enrico. Copper Nanoparticle/Polymer Composites with Antifungal and Bacteriostatic Properties. Chemistry of Materials, 2005; 17: 5255-5262.
16. Zhang, Hanlu, Cao, Jingyi, Sun, Li, Kong, Fabao, Tang, Jianhua, Zhao, Xuhui, Tang, Yuming and Zuo, Yu. Comparative Study on the Degradation of Two Self-Polishing Antifouling Coating Systems with Copper-Based Antifouling Agents. Coatings, 2022; 12: 1156.
17. Pérez-Alvarez, Marissa, Cadenas-Pliego, Gregorio, Pérez-Camacho, Odilia, Comparán-Padilla, Víctor E., Cabello-Alvarado, Christian J. and Saucedo-Salazar, Esmeralda. Green Synthesis of Copper Nanoparticles Using Cotton. Polymers, 2021; 13: 1906.
18. Sierra-Ávila, Rubén, Pérez-Alvarez, Marissa, Valdez-Garza, Janett, Avila-Orta, Carlos Alberto, Jiménez-Regalado, Enrique Javier, Mata-Padilla, José M., Soto-Castruita, Enrique and Cadenas-Pliego, Gregorio. Synthesis and Thermomechanical Characterization of Nylon 6/Cu Nanocomposites Produced by an Ultrasound-Assisted Extrusion Method. Advances in Materials Science and Engineering, 2018; 2018: 4792735.
19. Medellín-Banda, Diana Iris, Navarro-Rodríguez, Dámaso, Fernández-Tavizón, Salvador, Ávila-Orta, Carlos Alberto, Cadenas-Pliego, Gregorio and Comparán-Padilla, Victor Eduardo. Enhancement of the thermal conductivity of polypropylene with low loadings of CuAg alloy nanoparticles and graphene nanoplatelets. Materials Today Communications, 2019; 21: 100695.
20. Jardón-Maximino, Noemi, Cadenas-Pliego, Gregorio, Ávila-Orta, Carlos A., Comparán-Padilla, Víctor Eduardo, Lugo-Uribe, Luis E., Pérez-Alvarez, Marissa, Tavizón, Salvador Fernández and Santillán, Gerardo de Jesús Sosa. Antimicrobial Property of Polypropylene Composites and Functionalized Copper Nanoparticles. Polymers, 2021; 13: 1694.
21. Cota-Ungson, Diana, González-García, Yolanda, Cadenas-Pliego, Gregorio, Alpuche-Solís, Ángel Gabriel, Benavides-Mendoza, Adalberto and Juárez-Maldonado, Antonio. Graphene & ndash ; Cu Nanocomposites Induce Tolerance against Fusarium oxysporum, Increase Antioxidant Activity, and Decrease Stress in Tomato Plants. Plants, 2023; 12: 2270.
22. Montaño-Herrera, Anay, Santiago-Saenz, Yair Olovaldo, López-Palestina, César Uriel, Cadenas-Pliego, Gregorio, Pinedo-Guerrero, Zeus H., Hernández-Fuentes, Alma Delia and Pinedo-Espinoza, José Manuel. Effects of Edaphic Fertilization and Foliar Application of Se and Zn Nanoparticles on Yield and Bioactive Compounds in Malus domestica L. Horticulturae, 2022; 8: 542.
23. Sariñana-Navarrete, María de los Ángeles, Morelos-Moreno, Álvaro, Sánchez, Esteban, Cadenas-Pliego, Gregorio, Benavides-Mendoza, Adalberto and Preciado-Rangel, Pablo. Selenium Nanoparticles Improve Quality, Bioactive Compounds and Enzymatic Activity in Jalapeño Pepper Fruits. Agronomy, 2023; 13: 652.
24. Kong, Huiling, Yang, Jixin, Zhang, Yifeng, Fang, Yapeng, Nishinari, Katsuyoshi and Phillips, Glyn O. Synthesis and antioxidant properties of gum arabic-stabilized selenium nanoparticles. International Journal of Biological Macromolecules, 2014; 65: 155-162.
25. Bisht, Neha, Phalswal, Priyanka and Khanna, Pawan K. Selenium nanoparticles: a review on synthesis and biomedical applications. Materials Advances, 2022; 3: 1415-1431.
26. Khurana, A., Tekula, S., Saifi, M. A., Venkatesh, P. and Godugu, C. Therapeutic applications of selenium nanoparticles. Biomed Pharmacother, 2019; 111: 802-812.
27. Zhang, Aiyu, Ma, Qian, Wang, Zhaoguang, Lu, Mengkai, Yang, Ping and Zhou, Guangjun. Controllable synthesis of copper selenide nanocrystals through a green paraffin-acetate method. Materials Chemistry and Physics, 2010; 124: 916-921.
28. Hussain, Raja Azadar and Hussain, Iqtadar. Copper selenide thin films from growth to applications. Solid State Sciences, 2020; 100: 106101.

29. Shitu, Ibrahim Garba, Talib, Zainal Abidin, Chi, Josephine Liew Ying, Kechick, Mohd Mustapha Awang and Baqiah, Hussein. Influence of tartaric acid concentration on structural and optical properties of CuSe nanoparticles synthesized via microwave assisted method. Results in Physics, 2020; 17: 103041.
30. Liu, Kegao, Jing, Mingxing, Zhang, Li, Li, Jing and Shi, Lei. Characterization of the phases and morphology in synthesizing Cu_2-xSe and CuSe films. Integrated Ferroelectrics, 2018; 189: 71-77.
31. Hasanzadeh, Iraj, Barikani, Mehdi and Mahdavian, Ali Reza. Ultrasound-assisted emulsion polymerization of poly(methyl methacrylate-co-butyl acrylate): Effect of initiator content and temperature. Polymer Engineering & Science, 2016; 56: 214-221.
32. Avcı, Merih Zeynep and Sarac, A. Sezai. Transparent poly(methyl methacrylate-co-butyl acrylate) nanofibers. Journal of Applied Polymer Science, 2013; 130: 4264-4272.
33. Avc MZ, Sarac AS (2013) Transparent poly (methyl methacrylate-co-butyl acrylate) nanofibers. J Appl Polym Sci 130:4264–4272. https://doi.org/10.1002/app.39705
34. Al-Ansari, Mysoon M., Al-Dahmash, Nora D. and Ranjitsingh, A. J. A. Synthesis of silver nanoparticles using gum Arabic: Evaluation of its inhibitory action on Streptococcus mutans causing dental caries and endocarditis. Journal of Infection and Public Health, 2021; 14: 324-330.
35. Sandoval, P.; Baena, Y.; Aragón, M.; Rosas, J.; Ponce, L. Overall Mechanisms that Rule the Active Pharmaceutical Ingredient´s Delivery Process from Hydrophilic Matrices Elaborated with Ether Cellulose. Revista Colombiana de Ciencias Químico Farmacéuticas., 2008; 37: 105- 121.
36. Caro, F.; López, L.; Mendoza, J.; Monal W.; Goycoolea, F.; Carvajal, E.; López, Y. Métodos de Preparación de Nanopartículas de Quitosano: Una Revisión. Biotecnia, 2019; 11: 13- 25.
37. Kumari, Avnesh, Yadav, Sudesh Kumar and Yadav, Subhash C. Biodegradable polymeric nanoparticles based drug delivery systems. Colloids and Surfaces B: Biointerfaces, 2010; 75: 1-18.
38. Calderón, L.; Lecumberri, E.; Harris, R.; López, M.; Acosta, N.; Heras, A. Chemical Properties of Chitosan as a Marine Cosmeceutical. Marine Cosmeceuticals Trends and Prospects. 2011. 39- 51
39. Aragón, J.; González, R.; Fuentes, G. Cinética de Liberación de Cefalexiana desde un Biomaterial Compuesto por HAP-200/POVIAC/$CaCO_3$. Acad. Nac. Farm., 2009; 75: 345- 363.
40. Tian, Ye and Jiang, Lei. Intrinsically robust hydrophobicity. Nature Materials, 2013; 12: 291-292.